Low-dose CT Allows for Accurate Proton Therapy Dose Calculation and Plan Optimization

Masoud Elhamiasl[1] & Koen Salvo[2] & Kenneth Poels[2] & Gilles Defraene[3] & Maarten Lambrecht[2] & Xavier Geets[4,5] & Edmond Sterpin[3,5] & Johan Nuyts[1]

[1] Department of Imaging and Pathology, Division of Nuclear Medicine and Molecular Imaging, KU Leuven, Leuven, Belgium.
[2] Department of Radiotherapy Oncology, University Hospitals Leuven, Leuven, Belgium.
[3] Department of Oncology, Laboratory of Experimental Radiotherapy, KU Leuven, Leuven, Belgium.
[4] Department of Radiation Oncology, Cliniques universitaires Saint-Luc, Brussels, Belgium.
[5] Molecular Imaging, Radiotherapy and Oncology, Institut de Recherche Expérimentale et Clinique, UCLouvain, Brussels, Belgium.

E-mail: masoud.elhamiasl@kuleuven.be

Abstract. *Objective.* Protons offer a more conformal dose delivery compared to photons, yet they are sensitive to anatomical changes over the course of treatment. To minimize range uncertainties due to anatomical variations, a new CT acquisition at every treatment session would be paramount to enable daily dose calculation and subsequent plan adaptation. However, the series of CT scans results in an additional accumulated patient dose. Reducing CT radiation dose and thereby decreasing the potential risk of radiation exposure to patients is desirable, however, lowering the CT dose results in a lower signal-to-noise ratio and therefore in a reduced quality image. We hypothesized that the signal-to-noise ratio provided by conventional CT protocols is higher than needed for proton dose distribution estimation. In this study, we aim to investigate the effect of CT imaging dose reduction on proton therapy dose calculations and plan optimization. *Approach.* To verify our hypothesis, a CT dose reduction simulation tool has been developed and validated to simulate lower-dose CT scans from an existing standard-dose scan. The simulated lower-dose CTs were then used for proton dose calculation and plan optimization and the results were compared with those of the standard-dose scan. The same strategy was adopted to investigate the effect of CT dose reduction on water equivalent thickness (WET) calculation to quantify CT noise accumulation during integration along the beam. *Main results.* The similarity between the dose distributions acquired from the low-dose and standard-dose CTs was evaluated by the dose-volume histogram (DVH) and the 3D Gamma analysis. The results on an anthropomorphic head phantom and three patient cases indicate that CT imaging dose reduction up to 90% does not have a significant effect on proton dose calculation and plan optimization. The relative error was employed to evaluate the similarity between WET maps and was found to be less than 1% after reducing the CT imaging dose by 90%. *Significance.* The results suggest the possibility of using low-dose CT for proton therapy dose estimation, since the dose distributions acquired from the standard-dose and low-dose CTs are clinically equivalent.

Keywords: adaptive proton therapy, low-dose CT, dose calculation, plan optimization, protocol optimization.

1. Introduction

Proton therapy is an advanced form of external beam radiotherapy which utilizes high-energy proton beams to kill cancer cells. Compared to photons, protons offer a better localized dose deposition which enables the delivery of a highly conformal dose to the tumor while minimizing the damage to the surrounding healthy tissue, yet they are sensitive to anatomical variations. The total therapeutic radiation dose is typically split up into several tens of smaller fractions over the course of treatment, from several days to weeks (Sonke et al. 2019, Paganetti 2017). Anatomical changes frequently occur over the course of treatment, therefore, the delivered dose might differ from what was originally planned. Anatomical changes can occur in any region due to tumor shrinkage, weight loss, organ motion, variation in organ filling, etc. For example, shifts up to 5 mm between the tumor borders have been reported for patients who underwent stereotactic radiosurgery for brain metastases (Hessen et al. 2017). In esophageal cancer radiotherapy, shift up to more than 1 cm was observed in cranio-caudal direction, for distal locations (Thomas et al. 2021). Interested readers are referred to (Sonke et al. 2019) for a detailed examination of anatomical changes over the course of treatment.

Day-to-day anatomical variations can substantially compromise the properties of proton beams (Lomax 2008). That is due to the fact that the stopping power of the tissues traversed by the protons can vary substantially, and even relatively small changes of the trajectory of the protons through the body can have an important effect on the position of the Bragg peak. Research has shown that around one-third of proton patients required one or more repeated CT scans to adapt the plan during the course of treatment (Placidi et al. 2017). Applying a safety margin around the clinical target volumes or using robust optimization is necessary to account for the anatomical changes and ensuring coverage of the target. However, surrounding tissue will be exposed to higher levels of radiation, increasing the risk of side effects such as secondary malignancy. Image-guided proton therapy tries to reduce this margin by improving the set-up accuracy, however, the anatomical changes cannot be taken into account by translational and rotational setup corrections (Bertholet et al. 2020, Sonke et al. 2019). Adaptive Proton Therapy (APT) could be employed to detect these changes and adapt the plan if it is necessary.

APT aims to deliver radiation dose accurately in the presence of anatomical changes by employing a closed-loop imaging system to systematically monitor these changes and modify the treatment plan if required (Albertini et al. 2020). APT has been shown to have the advantage of reducing the safety margin compared to conventional image-guided approaches (Nenoff et al. 2020, Acharya et al. 2021, Geng et al. 2020). By enabling detection of and correction for changes, APT has the potential to improve

the quality of treatment by reducing Organ At Risks (OARs) exposure and toxicity and also facilitating dose escalation and therefore improved tumor control. A survey in 2019 showed that two thirds of radiotherapy centers worldwide are willing to implement adaptive approach for at least one new tumor site (Anastasi et al. 2020, Bertholet et al. 2020).

In-room or off-room CT, Cone Beam CT (CBCT), and on-board MR are the main modalities that can be used for APT. CT is the most accurate modality for estimating stopping powers, and provides also adequate contrast for image delineation. In the current state-of-the-art of the imaging device, the systematic acquisition of a CT image using an in-room CT would provide the best accuracy for dose calculation and subsequent plan adaptation (Lomax et al. 2020). A new CT scan directly before each treatment session would be paramount in order to exploit the full potential of proton therapy. Even though the dose from a CT is small compared to the therapeutic radiation, the total dose associated with the series of these CTs can be significant (Perks et al. 2008), especially if a 4D CT is acquired to account for breathing effects. This is highly relevant for children due to their longer life expectancy and susceptibility to mutagenesis (De Jong et al. 2014, Hess et al. 2016, Mathews et al. 2013). For example, cumulative doses from 2–3 head CTs could almost triple the risk of brain tumors and 5–10 head CTs could triple the risk of leukaemia in the 10 years after the first scan for patients younger than 10 years (Pearce et al. 2012). Therefore, minimizing the ionising radiation doses from the imaging system is crucial to reduce the risk of radiation-induced malignancies (Sheppard et al. 2018).

Reducing CT dose is always desirable, however, lowering the radiation dose results in a lower signal-to-noise ratio and therefore in a reduced image quality which may deteriorate the diagnostic and therapeutic value of CT images. We hypothesize that the signal-to-noise ratio provided by conventional CT protocols is higher than needed for accurate proton therapy dose estimation. In this research, we aim to investigate the effect of CT imaging dose reduction on proton therapy dose estimation. It should be noted that the effect of CT dose reduction on segmenting the target volumes and OARs (image contouring) falls out of the scope of this paper.

The rest of this paper is structured as follows. Section 2 begins with describing the research method used in this study. Section 2.1 and 2.2 discuss the possible approaches to investigate the effect of reducing CT dose on proton therapy dose estimation, including the effect of CT dose reduction on dose calculation, plan optimization, and water equivalent thickness estimation. Experimental results are presented in Section 3, followed by a discussion in Section 4. Finally, some concluding remarks are drawn in Section 5.

2. Materials and Methods

In order to assess the effect of CT dose reduction on proton therapy dose estimation, it is crucial to have the standard-dose CT, acquired with a routine clinical protocol,

along with the corresponding LDCT images. The dose distributions can then be estimated from the LDCTs and compared with that of the standard-dose scan. It is not ethical to scan the same patient several times using different acquisition protocols to generate the standard and low-dose CT pairs. Anthropomorphic phantoms can be used instead (Nenoff et al. 2021), however, their clinical relevance is less. A more sophisticated strategy is to use a tool to generate realistic LDCTs from an existing standard-dose CT scan and use them for proton therapy dose calculation.

To verify our hypothesis and enable a patient-dependent reduction of the CT dose, a LDCT simulation tool was developed and validated (Elhamiasl & Nuyts 2020) to simulate realistic lower-dose CT scans from an existing standard-dose scan. This tool produces a virtual lower-dose scan by adding the appropriate amount of (position dependent and correlated) noise to the standard-dose scan. Several phantom studies with different acquisition protocols were performed on different CT scanners to evaluate the accuracy of the proposed model. The results demonstrated excellent accuracy in providing realistic LDCT where the texture and magnitude of the simulated noise matched the measurements. The interested reader is referred to (Elhamiasl & Nuyts 2020) for further details on the developed model.

LDCT simulation with a gradual reduction in dose using real patient data enables us to verify to what extent the CT dose can be sacrificed without losing any relevant information required for proton dose estimation. Several experiments have been designed to assess the possibility of using LDCTs for proton therapy application. Each test starts from a standard-dose CT image where the results based on this reference CT image will be used as ground truth. Then noise is added to the CT scan to emulate the effect of CT dose reduction, and the same test is repeated for the simulated LDCTs. Comparing the results with those of the standard-dose scan will quantify the effect of CT dose reduction. The possible approaches to analyze the effect of reducing CT dose are discussed in the following sections.

2.1. Dose Estimation Error

In this work, a Pencil Beam Scanning (PBS) technique is employed for proton dose delivery. For PBS, spot positions and spot weights are the machine parameters that define the plan. After defining the objectives and constraints, the Treatment Planning System (TPS) selects the spot positions and their initial weights and works backward to minimize the objective function by modifying the spot weights. The plan optimization is therefore an iterative process to find the optimum spot weights that minimize the objective function. At each iteration, the dose distribution is calculated from the CT image, spot positions, and spot weights from which the dose to ROIs and OARs could be identified.

The dose calculation step can be affected by the CT noise. Plan optimization, which is an iterative process, can also be severely affected by the higher level of CT noise in LDCTs. It is conceivable that the CT noise propagation effects are more damaging

during an iterative plan optimization than during a single dose calculation. In addition, the noise in the LDCTs can affect plan initialization. For these reasons, we consider two scenarios: the dose calculation error and planning optimization error. It is crucial to investigate the effect of CT noise on these two errors separately owing to the fact that the error of dose calculation might be compensated by the error in plan optimization, and vice versa.

2.1.1. Dose Calculation Error In this experiment, LDCTs are only used for proton dose calculation. It is crucial to make sure that the calculated dose is a close representation of the actual delivered dose to the patient. Any deviation from the actual dose could have a serious impact on the quality of treatment. After delineating the target volume and OARs and defining the beams, the plan is optimized on the standard-dose CT image (OptHigh). The dose distribution will be then recomputed on a set of LDCTs (CalcLow) using the same optimized plan and the results compared with that of the standard-dose scan (OptHigh-CalcHigh). In other words, this experiment examines the effect of reducing CT noise on dose calculation in only one iteration.

2.1.2. Plan Optimization Error The second experiment assesses the effect of CT dose reduction on the plan optimization in which the plan is reoptimized separately for each LDCT (OptLow) and the doses are calculated using the standard-dose scans (CalcHigh). The results are then compared with the reference dose distribution (OptHigh-CalcHigh). LDCTs can affect the optimizer, first, during plan initialization where the spot positions and their initial weights are chosen, and second, at each iteration where the dose distribution is calculated. It should be mentioned that dose calculation error and plan optimization error are not independent. The plan optimization is an iterative procedure and its error is mainly due to the small error during dose calculation at each iteration. In this test, we are interested to see if these small errors during dose calculation could drive the optimization to a wrong solution. It is worth mentioning that the plan optimization test can be easily affected by other sources of uncertainties during the optimization procedure where a slight change of initial conditions or a small variation at one iteration may lead to unpredictable changes in the optimized plan. Therefore, it is crucial to minimize other sources of variability as much as possible to focus on CT noise only.

To summarize, three dose distributions will be estimated for each case as follows:

- *OptHigh-CalcHigh*: The plan was optimized on the standard-dose CT. The final dose was also calculated on the standard-dose CT. OptHigh-CalcHigh represents the closest approximation of the delivered dose to the patient using the optimal plan, therefore, it will be considered as the ground truth for validating the other doses.
- *OptHigh-CalcLow*: The plan was optimized on the standard-dose CT, but the final dose was recalculated on the LDCT. OptHigh-CalcLow shows the effect of CT noise on dose calculation and is the most robust and reliable test.

- *OptLow-CalcHigh*: The plan was optimized on LDCT, and the final dose was recalculated on the standard-dose CT. OptLow-CalcHigh shows the effect of CT noise on plan optimization and represents the closest approximation of the delivered dose to the patient for cases in which the plan is optimized on LDCT.

We have not used OptLow-CalcLow, where the plan optimization and also the final dose calculation would be carried out on the LDCT. The dose distributions from this experiment are not useful because errors on dose calculations are likely to be compensated by errors during plan optimization, such that the final estimated dose could agree well with the reference dose, despite significant errors during plan optimization.

2.2. Water Equivalent Thickness Error

In proton therapy applications, the radiological thickness of a material is expressed in terms of Water Equivalent Thickness (WET). WET can be estimated by adding Stopping Power Ratio (SPR) values for each voxel along the beam. The integration process can be considered as a smoothing filter that could partially suppress the noise in the LDCTs. The CT noise is high frequency noise, which implies that there are negative noise correlations between neighboring pixels. Therefore, by integrating along beams, some of the noise will cancel out.

Integrating along a line is intrinsic to dose calculation and plan optimization tasks. Therefore, an alternative solution to analyze the effect of CT dose reduction is to compare WET maps acquired from the standard-dose and LDCTs. This test could therefore determine if the surviving noise after integration along the beam is strong enough to cause problems for proton therapy dose estimation.

In this work, RayStation TPS (RaySearch Laboratories, Sweden) is employed for treatment planning. In RayStation the CT-number [HU] of a voxel is first converted to mass density [g/cm^3] by a site-specific CT-to-mass density calibration curve. The mass density is then mapped to material by selecting one of the 55 predefined materials which has the closest mass density to the mass density of the voxel. Finally, the stopping power is calculated from the mass density of the voxel, the characteristics of the RayStation material (atomical composition, mean excitation energy) and the proton energy at the position of the voxel.

After converting the CT-numbers [HU] to SPRs, the WET can be estimated as the line integral of the SPR (Deffet et al. 2020). The WET maps acquired from the LDCTs can then be compared with that of the standard-dose CT to quantify the remaining noise after integration.

2.3. Patient Cases and Treatment Planning

One phantom and three clinical cases were used to analyze the effect of reducing CT dose on proton therapy dose estimation. In each case, the LDCTs with gradual reduction in dose were simulated by employing the in-house LDCT simulator. The dose distributions

and WET maps were then estimated for the LDCTs and the results were compared with the ground truth. The plans were defined by a radiation therapy technologist in RayStation V9B. The details of each case are as follows:

- *Case 1*: A realistic proton therapy head phantom (Proton Therapy Dosimetry Head, Model 731-HN) was scanned with a routine clinical protocol [Siemens SOMATOM Force, 120 kVp, 340 effective mAs, pitch: 0.55, pixel size: 0.51×0.51×2 mm, $CTDI_{vol}$: 51 mGy, Effective dose ≈ 5 mSv]. The brainstem was contoured and the Planning Target Volume (PTV) was defined like a horseshoe around the brainstem. An Intensity Modulated Proton Therapy (IMPT) plan with a typical setup of 4 beams [50°, 130°, 220°, and 300°] was used and a dose of 60 Gy RBE (30 fractions of 2 Gy RBE) was prescribed on the PTV.
- *Case 2*: A standard-dose 3DCT scan [Siemens SOMATOM EDGE, 120 kVp, 340 effective mAs, pitch: 0.55, pixel size: 0.58×0.58×1 mm, $CTDI_{vol}$: 48 mGy, Effective dose ≈ 5 mSv] of a brain metastases patient was used. An IMPT plan with two beams (260° and 310°) was generated and a dose of 27 Gy RBE (3 fractions of 9 Gy RBE) was prescribed on the PTV.
- *Case 3*: A standard-dose 4DCT scan [Siemens SOMATOM Drive, 120 kVp, 50 effective mAs, 10 breathing phases, pitch: 0.09, pixel size: 0.97×0.97×3 mm, $CTDI_{vol}$: 30 mGy, Effective dose ≈ 20 mSv] for an esophageal cancer patient was used. An IMPT plan with two posterior beams (150° and 180°) was generated with the average image of the standard-dose 4DCT as planning CT. A dose of 50.40 Gy RBE (28 fractions of 1.80 Gy RBE) was prescribed on the Internal Clinical Target Volume (iCTV) using robustness settings of 7 mm setup error and 2.6% range error.
- *Case 4*: A standard-dose CT scan [Siemens SOMATOM Drive, 120 kVp, 198 effective mAs, pitch: 1.2, pixel size: 1.52×1.52×3 mm, $CTDI_{vol}$: 13 mGy, Effective dose ≈ 8.5 mSv] of a patient with vertebral metastases was selected. An IMPT plan with three posterior beams (140°, 180°, and 220°) was generated and a dose of 27 Gy RBE (10 fractions of 2.7 Gy RBE) was prescribed on the PTV.

3. Results

Each test started by adding noise to the standard-dose scan to simulate the effect of CT dose reduction. LDCTs with 75%, 50%, 40%, 30%, 20%, and 10% of the tube load reported for the standard-dose CT were simulated. A new reconstruction was made using Siemens offline reconstruction software [ReconCT V14.2.0.40998]. Even though reducing the CT dose beyond 10% of the reference dose is theoretically possible, performing a clinical CT scan below that level is not; therefore, the scan with 10% of the reference CT dose was typically the minimum CT dose that the CT scanner accepted. Figure 1 represents the simulated LDCT images with the corresponding acquired standard-dose CT image for each case. It can be seen that the CT noise increases by reducing the CT imaging dose.

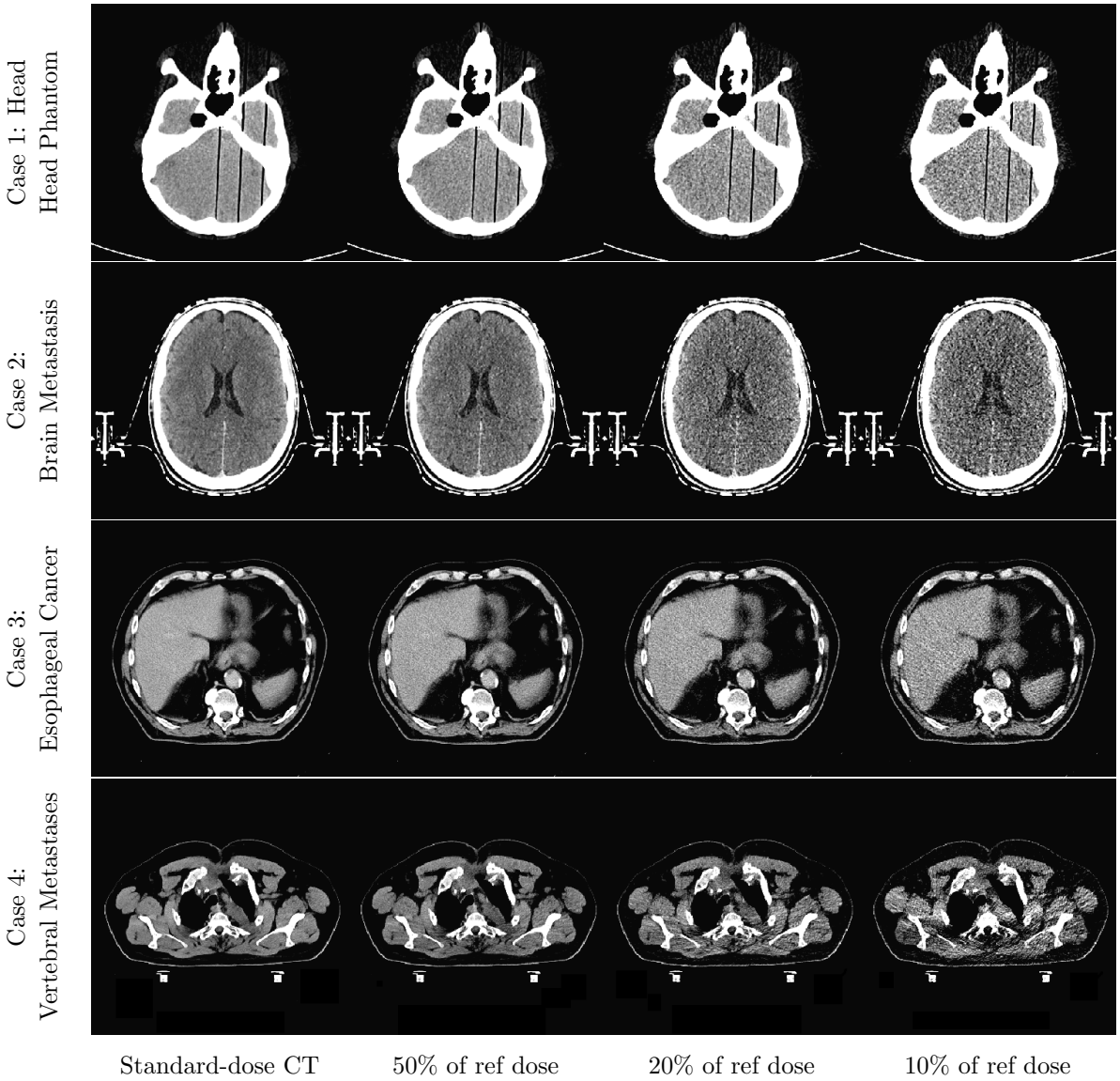

Figure 1: Representation of the standard-dose CT image (first column) and the corresponding simulated LDCTs (second, third, and fourth columns). It can be seen that the CT noise increases by lowering the CT dose.

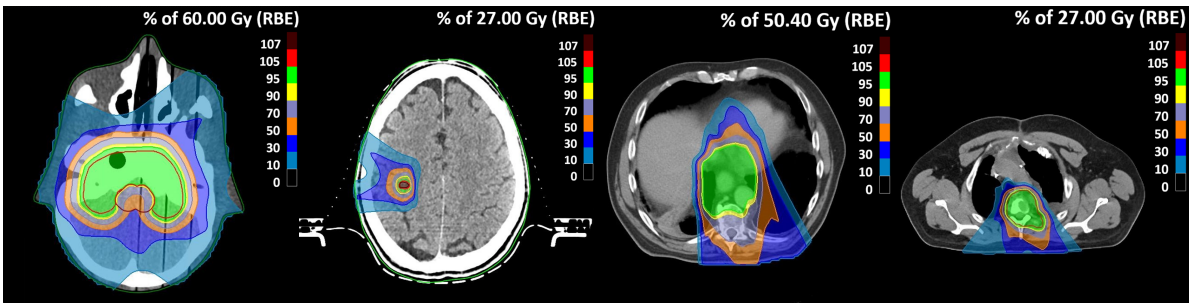

Figure 2: Axial slices of all the cases with overlaid dose distributions.

3.1. Dose Estimation Error

In the next step, the standard-dose CT image was used for dose calculation and plan optimization (OptHigh-CalcHigh) where the results based on this CT were considered as the ground truth. Figure 2 represents an axial slice of each case with overlaid estimated dose of OptHigh-CalcHigh. To minimize additional variation and focus on CT noise only, the same beam angle and same objective functions were used for the standard and LDCTs. In addition, a pencil beam engine was used for dose calculation and plan optimization to avoid additional variation due to the statistical uncertainty of a Monte Carlo simulation.

The dose distributions acquired from the standard-dose and low-dose CT images were compared using the Dose-Volume Histogram (DVH) and 3D Gamma analysis. The DVH provides valuable clinical information, but it does not carry spatial information about the dose distributions, for example, where the hot spots are located. To verify the spatial aspects, the local 3D Gamma analysis (Cohilis et al. 2019) was carried out over the region receiving at least 10% of the prescribed dose. The Gamma passing rate represents the percentage of voxels in the reference dose that have passed the test.

3.1.1. Dose Calculation Error In order to see the effect of CT noise on dose calculation, the plan was optimized on standard-dose CTs. The doses were then recomputed for the LDCTs using the same optimized plan (OptHigh-CalcLow) and the results were compared with that of the standard-dose scan (OptHigh-CalcHigh). For ease of reference, the term OptX-CalcY means that the plan was optimized on LDCT with X% of the reference dose (OptX) and the dose was recalculated for the LDCT with Y% of the reference dose (CalcY). The term High stands for the reference CT dose (standard-dose or high-dose scan).

Figure 3(a) compares OptHigh-CalcLow with OptHigh-CalcHigh using DVH analysis for case 3 (the DVHs for all other cases can be found in the supplementary materials, Figure S1). The DVHs are superimposed for target volume and OARs in all cases, showing the similarity between dose distributions calculated from the standard and LDCTs. The dose distributions were also compared using the Gamma analysis. Table 1 compares the dose distributions using the Gamma analysis using 3%/1mm and 1%/1mm criteria. Since the standard and low-dose CTs are perfectly aligned, a stricter measure of 1 mm distance-to-agreement was selected instead of the commonly selected 3 mm. The Gamma analysis also confirms the similarity between dose distributions where the mean value of the Gamma is much smaller than 1 and the Gamma passing rate is close to 100% in almost all the cases, except OptHigh-Dose10 in case 4. Having the Gamma passing rate close to 100% and also similar DVHs confirms that the effect of CT noise on proton dose calculation is not significant.

It can be seen that the Gamma values are higher for cases 3 and 4, compared to cases 1 and 2, which indicates a larger dose difference. It is due to the fact that different acquisition protocols were used for case 3 and 4 where the effective mAs was 50 mAs

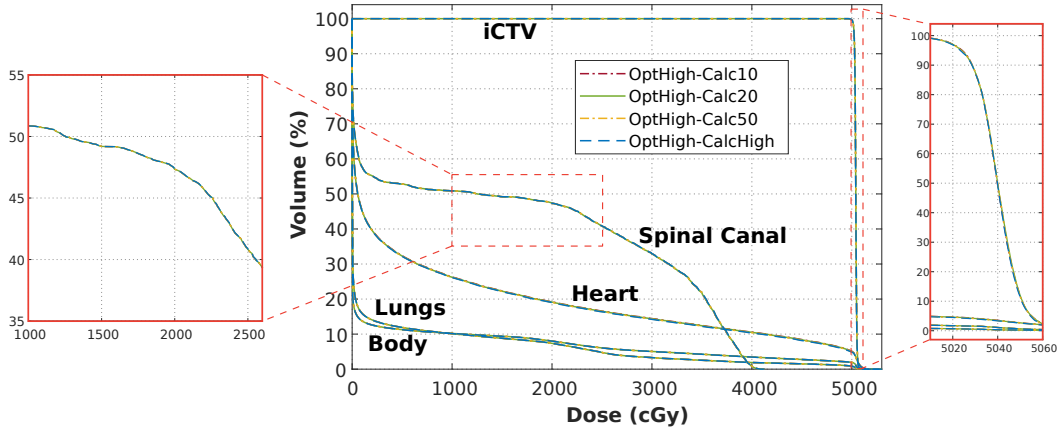

(a) Dose calculation test: OptHigh-CalcLow VS OptHigh-CalcHigh

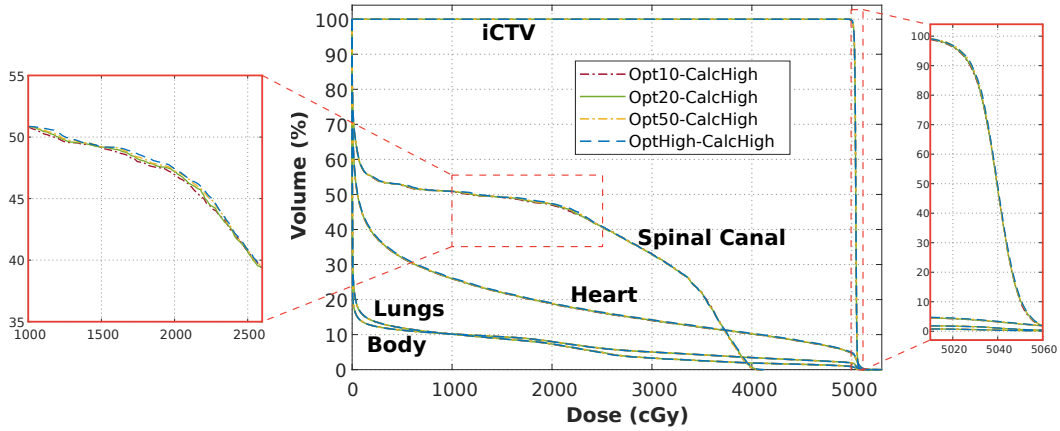

(b) Plan optimization test: OptLow-CalcHigh VS OptHigh-CalcHigh

Figure 3: Comparison of the DVHs for OARs and the target volume acquired from the standard and LDCTs to assess the effect of reducing CT imaging dose on (a) dose calculation and (b) plan optimization. Using LDCTs for dose calculation or plan optimization results in DVHs similar to the ground truth.

for case 3 and 192 mAs for case 4 compared to 340 mAs for cases 1 and 2. Therefore, the CT noise of the standard-dose CTs for cases 3 and 4 is higher than that of in cases 1 and 2, and therefore a larger error is expected.

3.1.2. Plan Optimization Error The LDCTs were also used for plan optimization where the plan was reoptimized on LDCTs and the dose calculation was carried out using the standard-dose scan (OptLow-CalcHigh). The main challenge in this test is that the plan can easily be affected by other sources of variability, such as different initial conditions. Figure 3(b) compares OptLow-CalcHigh with OptHigh-CalcHigh for case 3, showing the effect of CT dose reduction on plan optimization (the DVHs for all other cases is presented in the supplementary materials, Figure S2). The DVHs are aligned for the target volume and OARs. Table 2 compares the dose distributions using the Gamma

Table 1: Comparison of OptHigh-CalcLow with OptHigh-CalcHigh using the Gamma index passing rate (GPR %) and the mean value of the Gamma index, showing the effect of CT dose reduction on proton dose calculation (reference dose = OptHigh-CalcHigh).

		Case 1		Case 2		Case 3		Case 4	
	Evaluated Dose (%) ⇓	GPR	mean	GPR	mean	GPR	mean	GPR	mean
criteria: 3%, 1mm	OptHigh-Dose75	100	0.00	100	0.01	100	0.04	99.97	0.08
	OptHigh-Dose50	100	0.00	100	0.01	100	0.04	99.93	0.09
	OptHigh-Dose40	100	0.00	100	0.01	100	0.04	99.94	0.08
	OptHigh-Dose30	100	0.00	100	0.01	100	0.05	99.97	0.08
	OptHigh-Dose20	100	0.01	100	0.02	100	0.06	100	0.06
	OptHigh-Dose10	100	0.01	100	0.02	99.92	0.07	98.25	0.16
criteria: 1%, 1mm	OptHigh-Dose75	100	0.01	100	0.03	100	0.07	99.90	0.12
	OptHigh-Dose50	100	0.01	100	0.02	100	0.08	99.85	0.13
	OptHigh-Dose40	100	0.01	100	0.03	99.99	0.08	99.88	0.13
	OptHigh-Dose30	100	0.01	100	0.03	100	0.09	99.93	0.13
	OptHigh-Dose20	100	0.02	100	0.04	99.99	0.10	99.99	0.11
	OptHigh-Dose10	100	0.04	100	0.05	99.87	0.12	97.19	0.25

Table 2: Comparison of OptLow-CalcHigh with OptHigh-CalcHigh using the Gamma passing rate (GPR %) and the mean value of the Gamma index showing the effect of CT dose reduction on plan optimization (reference dose = OptHigh-CalcHigh).

		Case 1		Case 2		Case 3		Case 4	
	Evaluated Dose (%) ⇓	GPR	mean	GPR	mean	GPR	mean	GPR	mean
criteria: 3%, 1mm	Opt75-CalcHigh	99.99	0.14	100	0.06	97.06	0.22	97.93	0.24
	Opt50-CalcHigh	99.99	0.13	99.93	0.11	98.33	0.23	98.41	0.21
	Opt40-CalcHigh	99.99	0.13	100	0.05	97.20	0.23	97.42	0.22
	Opt30-CalcHigh	99.88	0.16	96.93	0.27	95.90	0.27	98.53	0.21
	Opt20-CalcHigh	99.94	0.15	99.94	0.14	96.34	0.26	97.42	0.22
	Opt10-CalcHigh	99.60	0.16	100	0.12	95.53	0.30	95.73	0.31
criteria: 1%, 1mm	Opt75-CalcHigh	98.63	0.26	100	0.11	92.24	0.41	94.57	0.37
	Opt50-CalcHigh	98.58	0.25	99.93	0.15	92.88	0.40	96.49	0.32
	Opt40-CalcHigh	99.17	0.24	100	0.10	92.51	0.42	95.70	0.35
	Opt30-CalcHigh	97.03	0.29	95.74	0.34	90.40	0.48	96.12	0.33
	Opt20-CalcHigh	98.77	0.26	99.88	0.18	91.60	0.46	94.73	0.35
	Opt10-CalcHigh	97.09	0.29	98.92	0.16	88.48	0.51	92.14	0.49

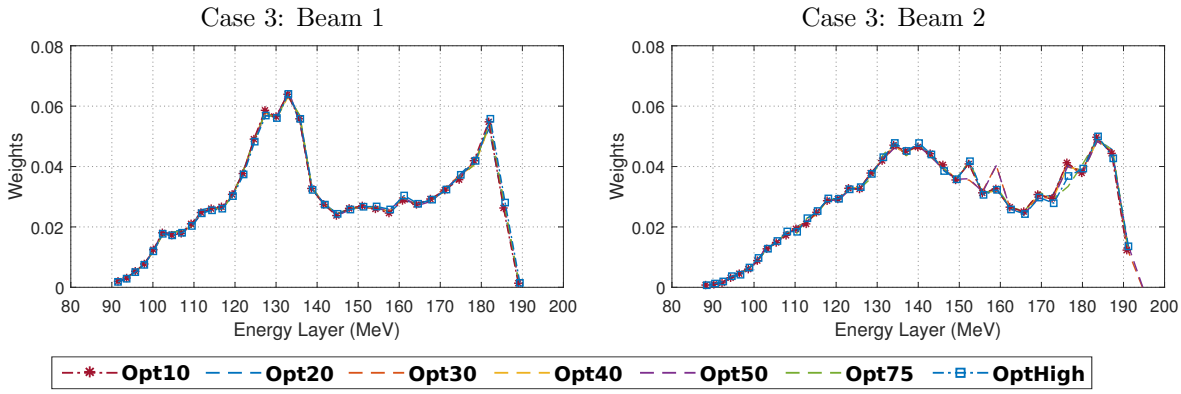

Figure 4: Representation of the energy layers and the corresponding relative weights for two beams in case 3. The plans were reoptimized on the standard-dose and LDCTs separately.

analysis. Typically, a clinical threshold of about 90% success for a 3%/3mm criterion is required to consider two dose distributions clinically equivalent (Ezzell et al. 2009). Considering 3%/1mm criteria, it can be seen that more than 95.50% of voxels passed the Gamma analysis which confirms that the dose distributions are clinically equivalent. It should be noted that the clinical goals were met in all cases and for all levels of CT dose.

An alternative way to compare the optimized plans can be achieved by comparing the energy layers and their corresponding relative weights for the plans optimized on LDCTs (OptLow) with those of the standard-dose scan (OptHigh). The relative weight is normalized within each beam and the total relative weight sums up to 100%. Figure 4 represents the energy layers (X axis) and the relative weights (Y axis) for two beams in case 3 (the energy layers and the relative weights for other cases is presented in the supplementary materials, Figure S3). It can be seen that there is a close agreement between the energy layers and their weight for the plans optimized on the standard-dose and LDCTs, suggesting the plans yield similar dose distributions.

Investigating the regions where the estimated dose differs from the ground truth suggests that the majority of the error occurs in those regions where the optimizer has the flexibility to modify the plan. Figure 5 shows the dose difference between Opt10-CalcHigh and OptHigh-CalcHigh and the corresponding Gamma index map for each case. It can be seen that the majority of the error occurs outside of the target volumes. In fact, in all plans, the objective functions were defined to make a conformal dose in the target volumes (objectives: max and min dose, uniform dose) and to minimize the dose to the OARs (objectives: max and mean dose). The plans were optimized based on these objectives, therefore, the optimizer is insensitive to the dose in non-ROI and non-OAR regions and the dose difference is more likely to be higher in these regions.

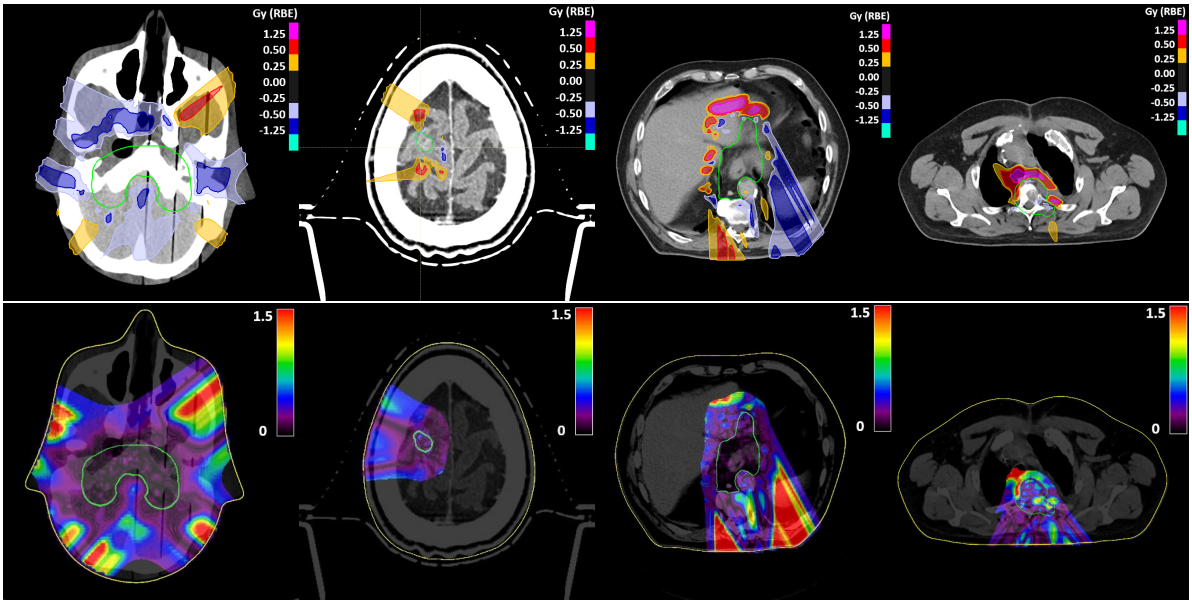

Figure 5: Representation of (first row) the difference between treatment dose acquired from OptHigh-CalcHigh and Opt10-CalcHigh and (second row) the corresponding Gamma index map for each case. The green contour represents the target volume. It can be seen that the majority of error occurs in non-ROI and non-OAR regions.

3.2. WET Estimation Error

WET maps were calculated using openPR plugin which is a part of openREGGUI, an open-source image processing platform for APT. Wet maps were calculated along the lateral direction (corresponding to gantry angles of 270°) for cases 1 and 2 and along the antero-posterior direction (corresponding to gantry angles of 180°) for cases 3 and 4 to resemble the commonly used beam angle for each case. Figure 6 represents the WET maps acquired from the standard and low-dose CTs and the corresponding relative error for case 3 for different levels of CT dose (the WET maps for other cases can be found in the supplementary materials, Figure S4). Table 3 reports the mean value of the relative and absolute error for WET maps. It can be seen that the relative and absolute error is smaller than 0.4% and 0.8 mm, respectively, confirming that the surviving noise after integration along the beam is small.

4. Discussion

The results show that reducing the CT dose does not have a significant effect on proton therapy dose estimation, even for the plans with non-robust optimization. Since robust plans should be less sensitive to the noise in the CT images, these three cases can be considered worst case scenarios. Therefore, the accumulated noise after integration along the beam does not adversely affect proton therapy dose calculations, even with

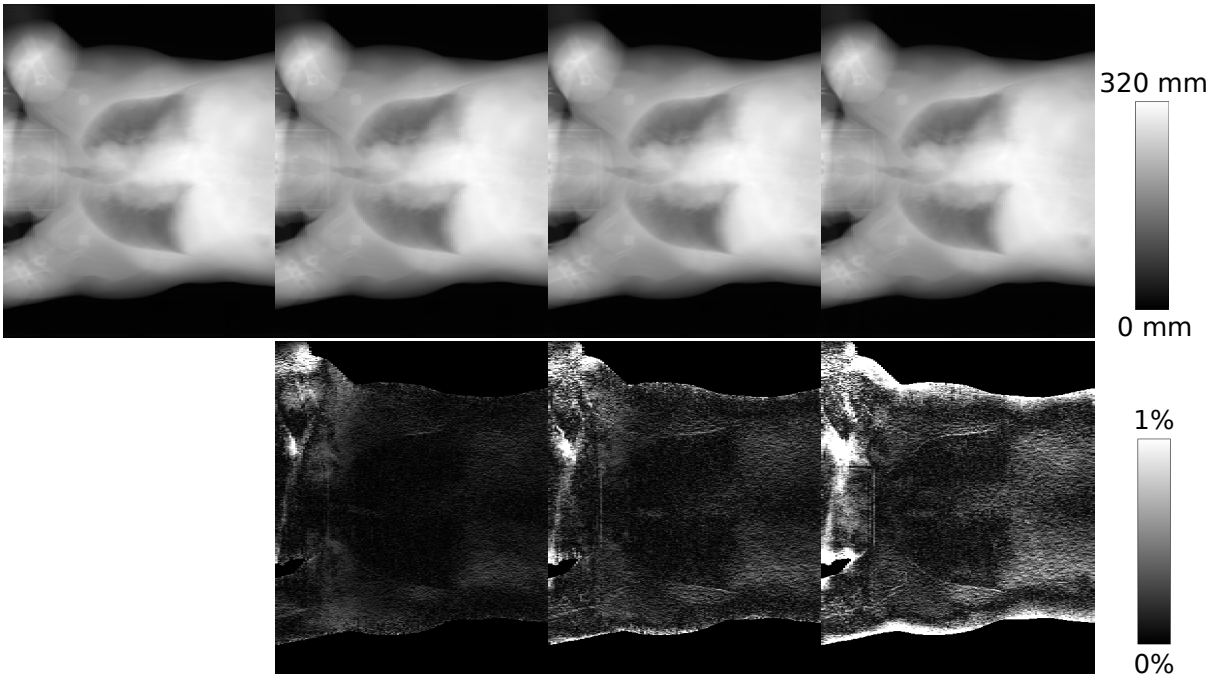

Figure 6: Representation of (first row) the WET maps calculated from the the standard-dose and LDCTs in case 3 and (second row) the corresponding relative error.

Table 3: Comparison of the WET maps estimated from the standard-dose and LDCTs using the mean value of the relative error (RE in %) and absolute error (AE in mm).

	Case 1		Case 2		Case 3		Case 4	
CT dose (%) ⇓	RE	AE	RE	AE	RE	AE	RE	AE
75% of ref dose	0.02	0.02	0.02	0.03	0.09	0.18	0.20	0.42
50% of ref dose	0.02	0.02	0.03	0.04	0.11	0.20	0.22	0.47
40% of ref dose	0.03	0.03	0.04	0.05	0.12	0.23	0.24	0.51
30% of ref dose	0.04	0.04	0.04	0.06	0.14	0.26	0.26	0.58
20% of ref dose	0.05	0.06	0.06	0.08	0.17	0.32	0.31	0.68
10% of ref dose	0.09	0.10	0.10	0.14	0.33	0.57	0.42	0.83

strong dose reductions. The reason is that the CT protocols have been optimized for imaging small CT-number [HU] differences at a high spatial resolution, because they are clinically relevant. A much stronger noise suppression (and higher resolution) is required for visualizing these small HU differences, than for ensuring quantitative accuracy of the proton dose computations.

The results suggest the possibility of using LDCTs for dose calculation. The DVH curves and Gamma analysis indicate that the dose distributions acquired from the

standard and low-dose CTs are equivalent. The Gamma passing rate is higher than 99.92% (3%,1mm) even after an aggressive dose reduction by a factor of up to 10, except for the LDCT with 10% of the reference dose in case 4. The dose calculation test is robust against other sources of variability and is a good representation of the effect of reducing CT dose. It can be seen that the mean of the Gamma value increased monotonically by lowering the CT dose.

The LDCTs can also be used for plan optimization, however, a larger error was observed. It could be due to several reasons: first, the CT noise slightly affected the spot positions and therefore the energy layers associated with the spot positions. Second, the CT noise propagation may be more damaging during several hundreds of consecutive iterations than during a single dose calculation. For example, the optimization algorithm may attribute a higher weight to beamlets that happen to look better than they are due to noise. Third, the risk of ending up in a local optimum is higher when the CT is noisier.

Using a pencil beam engine eliminated the variation due to Monte Carlo simulation, however, there are other sources of variation, such as different initial conditions. In order to minimize these variations, the same experiment was repeated by using different optimization settings. For example, the plans were reoptimized without spot filtering to make sure that no spot or energy layer will be removed during plan optimization. Spot filtering ensures that all spots are deliverable by removing spots with weights below the minimum deliverable monitor units (MUs). The absolute dose difference between OptLow-CalcHigh and OptHigh-CalcHigh decreased by a factor of 2 for all levels of LDCTs after reoptimizing the plans without spot filtering. In another experiment, the spot spacing for planning optimization was set to 0.5, instead of the default value of 1. The spot spacing defines the inter-spot distance, where a lower value decreases the inter-spot distance and therefore more spots would be engaged in a plan. It was seen that after increasing the number of spots and avoiding spot filtering the absolute dose difference was reduced by a factor of 4. The results proved that the plan optimization error is also affected by other sources of variability.

The fact that the Gamma passing rate hardly increases with increasing dose reduction in Table 2 supports the assumption that the optimized plan is affected by other variabilities. It can be seen that optimizing on LDCTs has a constant adverse effect on the Gamma passing rate of about 2% in case 1, 8% in case 3, and 5% in case 4 considering 1%,1mm criteria. Because the plan optimization error seems independent of the noise reduction, we attribute a portion of this error to arbitrary behavior of the optimization where, for example, a slight change of initial conditions or a small change in one iteration may lead to unpredictable changes in the optimized results. Thus, we believe that the observed error is also affected by other sources that are always present in clinical practice, implying that the CT noise increase has a negligible effect on the plan optimization.

Even though the error of plan optimization is larger than the dose calculation error, the LDCTs can still be used for plan optimization due to the fact that OptLow-CalcHigh

met all the clinical goals for all levels of LDCTs. The optimized plan on LDCT might differ from the ground truth but it does not necessarily mean that the optimized plan is incorrect. Plan optimization is not a single solution problem and there could be several plans that meet the clinical goal.

The WET maps also indicate that the accumulated error after integration along the beam is small. The relative error is smaller than 1% in the majority of regions except in high attenuated regions such as dental fillings. However, the dental filling region will be usually avoided for beams to travel through. There are two reasons for the higher error in these regions. In the high attenuated regions, the number of detected photons by the CT scanner can become very small, triggering the application of a smoothing filter by the acquisition software to suppress the CT noise. This smoothing filter results in the underestimation of the HU for high attenuated regions. In addition, the CT number-to-SPR conversion is piece-wise linear, therefore, the estimated proton stopping powers are a non-linear function of the reconstructed Hounsfield unit. A zero mean noise will be converted to non-zero mean noise by such non-linear conversion and a systematic error is expected, especially in those points where the slope of the curve varies a lot (Brousmiche et al. 2017). This nonlinearity along with the higher level of CT noise in the LDCTs resulted in the higher error.

The effect of reducing CT imaging dose on the delineation of the target volumes and OARs has not been discussed in this work. In APT, however, the generation of reliable new contours, together with their verification and approval for repeated images is crucial (Villarroel et al. 2020), yet, its implementation in clinical practice is challenging (LEE et al. 2020). Alternatively, simplified approaches such as dose restoration (Jagt et al. 2017, Bernatowicz et al. 2018, Villarroel et al. 2020) can be employed to facilitate the online adaptive workflow. Dose restoration aims to detect density changes along the beam path to reproduce the planned dose based on the new repeated images. In proton therapy, dose restoration is applicable when the change in anatomy is small and rigid mapping of contours from the previous CT image to the CT of the day is accurate. It generates a new restored plan by adapting proton beam energies and spot weights without involving contour adjustments in the workflow. This makes this work highly relevant for dose restoration approaches (Borderías-Villarroel et al. 2022, Bernatowicz et al. 2018, Villarroel et al. 2020) where the repeated CTs are used for plan adaptation without involving contour adjustments.

It was shown that the LDCTs are good enough for dose calculation but the noise might become problematic for the verification and correction of lesion and organ contours. Therefore the dose reductions may have to be less aggressive if the CT images are (also) used for organs and targets contouring tasks. The effect of reducing CT dose on image contouring will be investigated in future research. For the lesion and organ contouring, contouring experts will be asked to correct existing contours or define new contours, both on the standard-dose images and the reduced-dose images. In addition, an advanced convolutional neural network-based image denoising method (Yuan et al. 2020) is being developed to suppress the CT noise for organs

contouring tasks. The in-house LDCT simulator will be used to generate the standard-dose and low-dose pairs for training the model. The LDCTs can then be denoised for organ delineation tasks.

5. Conclusion

We hypothesized that the signal-to-noise ratio provided by conventional CT protocols is higher than needed for proton therapy dose estimation. To address this question, LDCTs were simulated from an existing standard-dose scan with a previously validated method. The LDCTs were used for dose estimation and the results were compared with that on the standard-dose scan. The results based on a phantom and three patient cases suggested that an aggressive CT imaging dose reduction by 90% does not have a significant effect on proton dose estimation. The DVH of the doses estimated from the standard-dose and LDCTs were on top of each other. The Gamma analysis also showed that the doses are clinically equivalent. The WET maps calculated from the LDCT images were in close agreement with that of the standard-dose CT.

Acknowledgments

This project is supported by Fonds Baillet-Latour. Gilles Defraene is postdoctoral fellow of the Research Foundation Flanders (FWO, project 1292021).

Ethical Statement

The ethics committee research of University Hospital Leuven (UZ Leuven) has approved the research (Reference Number: S66614, S65639, and S59667).

The research was conducted in accordance with the principles embodied in the Declaration of Helsinki and in accordance with local statutory requirements. All participants (or their parent or legal guardian in the case of children under 16) gave written informed consent to participate in the study.

References

Acharya S, Wang C, Quesada S, Gargone M A, Ates O, Uh J, Krasin M J, Merchant T E & ho Hua C 2021 Adaptive proton therapy for pediatric patients: Improving the quality of the delivered plan with on-treatment MRI *International Journal of Radiation Oncology*Biology*Physics* **109**(1), 242–251.
URL: *https://doi.org/10.1016/j.ijrobp.2020.08.036*

Albertini F, Matter M, Nenoff L, Zhang Y & Lomax A 2020 Online daily adaptive proton therapy *The British Journal of Radiology* **93**(1107), 20190594.
URL: *https://doi.org/10.1259/bjr.20190594*

Anastasi G, Bertholet J, Poulsen P, Roggen T, Garibaldi C, Tilly N, Booth J T, Oelfke U, Heijmen B & Aznar M C 2020 Patterns of practice for adaptive and real-time radiation therapy (POP-ART

RT) part i: Intra-fraction breathing motion management *Radiotherapy and Oncology* **153**, 79–87.
URL: *https://doi.org/10.1016/j.radonc.2020.06.018*

Bernatowicz K, Geets X, Barragan A, Janssens G, Souris K & Sterpin E 2018 Feasibility of online IMPT adaptation using fast, automatic and robust dose restoration *Physics in Medicine & Biology* **63**(8), 085018.
URL: *https://doi.org/10.1088/1361-6560/aaba8c*

Bertholet J, Anastasi G, Noble D, Bel A, van Leeuwen R, Roggen T, Duchateau M, Pilskog S, Garibaldi C, Tilly N, García-Mollá R, Bonaque J, Oelfke U, Aznar M C & Heijmen B 2020 Patterns of practice for adaptive and real-time radiation therapy (POP-ART RT) part II: Offline and online plan adaption for interfractional changes *Radiotherapy and Oncology* **153**, 88–96.
URL: *https://doi.org/10.1016/j.radonc.2020.06.017*

Borderías-Villarroel E, Taasti V, Elmpt W V, Teruel-Rivas S, Geets X & Sterpin E 2022 Evaluation of the clinical value of automatic online dose restoration for adaptive proton therapy of head and neck cancer *Radiotherapy and Oncology* .
URL: *https://doi.org/10.1016/j.radonc.2022.03.011*

Brousmiche S, Souris K, de Xivry J O, Lee J A, Macq B & Seco J 2017 Combined influence of CT random noise and HU-RSP calibration curve nonlinearities on proton range systematic errors *Physics in Medicine & Biology* **62**(21), 8226–8245.
URL: *https://doi.org/10.1088/1361-6560/aa86e9*

Cohilis M, Sterpin E, Lee J A & Souris K 2019 A noise correction of the γ-index method for monte carlo dose distribution comparison *Medical Physics* **47**(2), 681–692.
URL: *https://doi.org/10.1002/mp.13888*

De Jong R, Lens E, Van Herk M, Alderliesten T, Kamphuis M, Fajardo R D, Bel A & Van Wieringen N 2014 Oc-0282: Optimizing cone-beam ct presets for children to reduce imaging dose illustrated with craniospinal axis *Radiotherapy and Oncology* (111), S109–S110.

Deffet S, Cohilis M, Souris K, Salvo K, Depuydt T, Sterpin E & Macq B 2020 openPR — a computational tool for CT conversion assessment with proton radiography *Medical Physics* **48**(1), 387–396.
URL: *https://doi.org/10.1002/mp.14571*

Elhamiasl M & Nuyts J 2020 Low-dose x-ray CT simulation from an available higher-dose scan *Physics in Medicine & Biology* **65**(13), 135010.
URL: *https://doi.org/10.1088/1361-6560/ab8953*

Ezzell G A, Burmeister J W, Dogan N, LoSasso T J, Mechalakos J G, Mihailidis D, Molineu A, Palta J R, Ramsey C R, Salter B J, Shi J, Xia P, Yue N J & Xiao Y 2009 IMRT commissioning: Multiple institution planning and dosimetry comparisons, a report from AAPM task group 119 *Medical Physics* **36**(11), 5359–5373.
URL: *https://doi.org/10.1118/1.3238104*

Geng C, Han Y, Tang X, Shu D, Gong C & Altieri S 2020 Evaluation of using the doppler shift effect of prompt gamma for measuring the carbon ion range in vivo for heterogeneous phantoms *Nuclear Instruments and Methods in Physics Research Section A: Accelerators, Spectrometers, Detectors and Associated Equipment* **959**, 163439.
URL: *https://doi.org/10.1016/j.nima.2020.163439*

Hess C B, Thompson H M, Benedict S H, Seibert J A, Wong K, Vaughan A T & Chen A M 2016 Exposure risks among children undergoing radiation therapy: Considerations in the era of image guided radiation therapy *International Journal of Radiation Oncology*Biology*Physics* **94**(5), 978–992.
URL: *https://doi.org/10.1016/j.ijrobp.2015.12.372*

Hessen E D, van Buuren L D, Nijkamp J A, de Vries K C, Mok W K, Dewit L, van Mourik A M, Berlin A, van der Heide U A & Borst G R 2017 Significant tumor shift in patients treated with stereotactic radiosurgery for brain metastasis *Clinical and Translational Radiation Oncology*

2, 23–28.
URL: *https://doi.org/10.1016/j.ctro.2016.12.007*

Jagt T, Breedveld S, van de Water S, Heijmen B & Hoogeman M 2017 Near real-time automated dose restoration in IMPT to compensate for daily tissue density variations in prostate cancer *Physics in Medicine and Biology* **62**(11), 4254–4272.
URL: *https://doi.org/10.1088/1361-6560/aa5c12*

LEE V S C, SchettIno G & Nisbet A 2020 UK adaptive radiotherapy practices for head and neck cancer patients *BJR|Open* **2**(1), 20200051.
URL: *https://doi.org/10.1259/bjro.20200051*

Lomax A J 2008 Intensity modulated proton therapy and its sensitivity to treatment uncertainties 1: the potential effects of calculational uncertainties *Physics in Medicine and Biology* **53**(4), 1027–1042.
URL: *https://doi.org/10.1088/0031-9155/53/4/014*

Lomax T, Bolsi A & Albertini F 2020 Adaptive proton therapy utilizing an in-room ct *Siemens Healthineers White Paper* .

Mathews J D, Forsythe A V, Brady Z, Butler M W, Goergen S K, Byrnes G B, Giles G G, Wallace A B, Anderson P R, Guiver T A, McGale P, Cain T M, Dowty J G, Bickerstaffe A C & Darby S C 2013 Cancer risk in 680 000 people exposed to computed tomography scans in childhood or adolescence: data linkage study of 11 million australians *BMJ* **346**(may21 1), f2360–f2360.
URL: *https://doi.org/10.1136/bmj.f2360*

Nenoff L, Matter M, Charmillot M, Krier S, Uher K, Weber D C, Lomax A J & Albertini F 2021 Experimental validation of daily adaptive proton therapy *Physics in Medicine & Biology* **66**(20), 205010.
URL: *https://doi.org/10.1088/1361-6560/ac2b84*

Nenoff L, Matter M, Jarhall A G, Winterhalter C, Gorgisyan J, Josipovic M, Persson G F, af Rosenschold P M, Weber D C, Lomax A J & Albertini F 2020 Daily adaptive proton therapy: Is it appropriate to use analytical dose calculations for plan adaption? *International Journal of Radiation Oncology*Biology*Physics* **107**(4), 747–755.
URL: *https://doi.org/10.1016/j.ijrobp.2020.03.036*

Paganetti H 2017 *Proton Beam Therapy* 2399-2891 IOP Publishing.
URL: *http://dx.doi.org/10.1088/978-0-7503-1370-4*

Pearce M S, Salotti J A, Little M P, McHugh K, Lee C, Kim K P, Howe N L, Ronckers C M, Rajaraman P, Craft A W, Parker L & de González A B 2012 Radiation exposure from CT scans in childhood and subsequent risk of leukaemia and brain tumours: a retrospective cohort study *The Lancet* **380**(9840), 499–505.
URL: *https://doi.org/10.1016/s0140-6736(12)60815-0*

Perks J R, Lehmann J, Chen A M, Yang C C, Stern R L & Purdy J A 2008 Comparison of peripheral dose from image-guided radiation therapy (IGRT) using kV cone beam CT to intensity-modulated radiation therapy (IMRT) *Radiotherapy and Oncology* **89**(3), 304–310.
URL: *https://doi.org/10.1016/j.radonc.2008.07.026*

Placidi L, Bolsi A, Lomax A J, Schneider R A, Malyapa R, Weber D C & Albertini F 2017 Effect of anatomic changes on pencil beam scanned proton dose distributions for cranial and extracranial tumors *International Journal of Radiation Oncology* Biology* Physics* **97**(3), 616–623.

Sheppard J P, Nguyen T, Alkhalid Y, Beckett J S, Salamon N & Yang I 2018 Risk of brain tumor induction from pediatric head CT procedures: A systematic literature review *Brain Tumor Research and Treatment* **6**(1), 1.
URL: *https://doi.org/10.14791/btrt.2018.6.e4*

Sonke J J, Aznar M & Rasch C 2019 Adaptive radiotherapy for anatomical changes *Seminars in Radiation Oncology* **29**(3), 245–257.
URL: *https://doi.org/10.1016/j.semradonc.2019.02.007*

Thomas M, Roover R D, van der Merwe S, Lambrecht M, Defraene G & Haustermans K 2021 The

use of tumour markers in oesophageal cancer to quantify setup errors and baseline shifts during treatment *Clinical and Translational Radiation Oncology* **26**, 8–14.
URL: *https://doi.org/10.1016/j.ctro.2020.11.001*

Villarroel E B, Geets X & Sterpin E 2020 Online adaptive dose restoration in intensity modulated proton therapy of lung cancer to account for inter-fractional density changes *Physics and Imaging in Radiation Oncology* **15**, 30–37.
URL: *https://doi.org/10.1016/j.phro.2020.06.004*

Yuan N, Zhou J & Qi J 2020 Half2half: deep neural network based CT image denoising without independent reference data *Physics in Medicine & Biology* **65**(21), 215020.
URL: *https://doi.org/10.1088/1361-6560/aba939*

Supplementary Materials

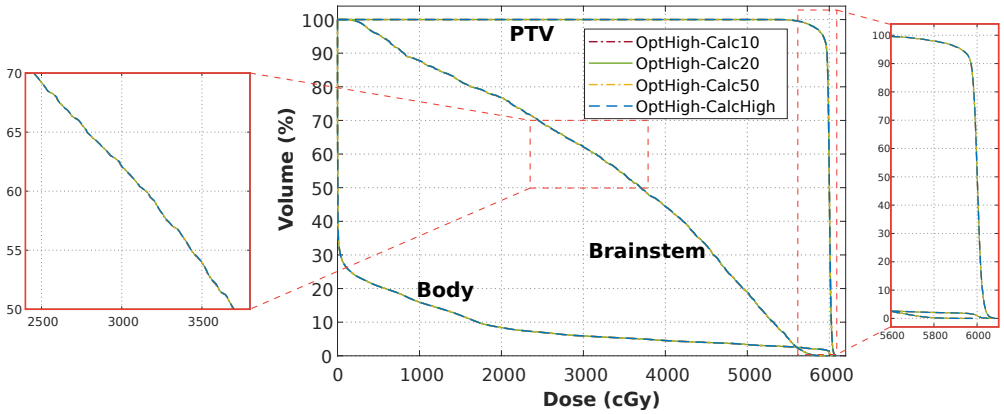

Case 1: Head Phantom

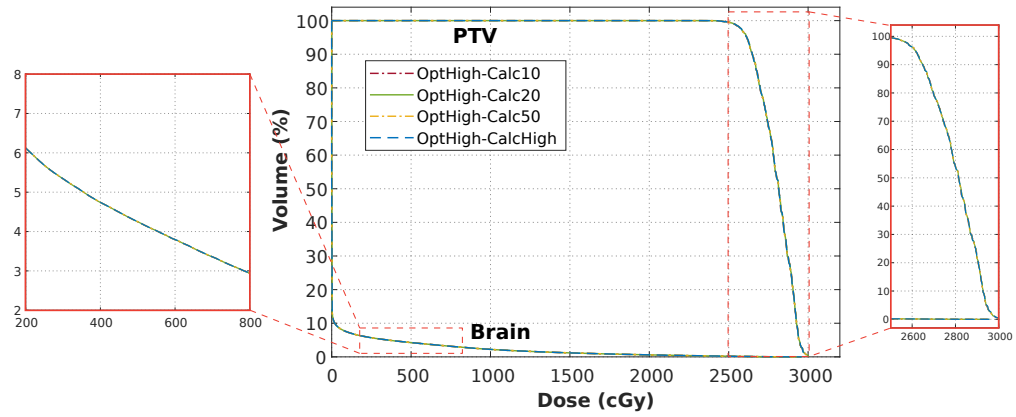

Case 2: Brain Metastasis

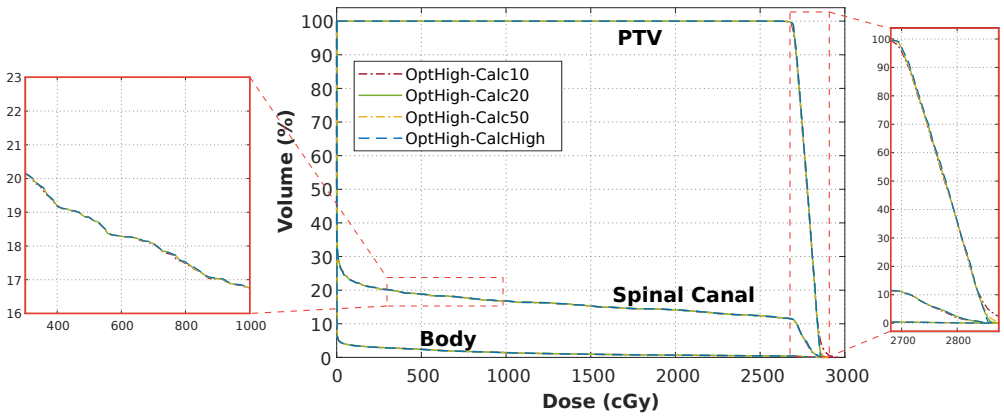

Case 4: Vertebral Metastases

Figure S1: Comparison of the DVHs for organs at risk and the target volume acquired from the standard and LDCTs showing the effect of CT dose reduction on dose calculation (OptHigh-CalcLow VS OptHigh-CalcHigh). Using LDCTs for dose calculation resulted in DVHs similar to the ground truth.

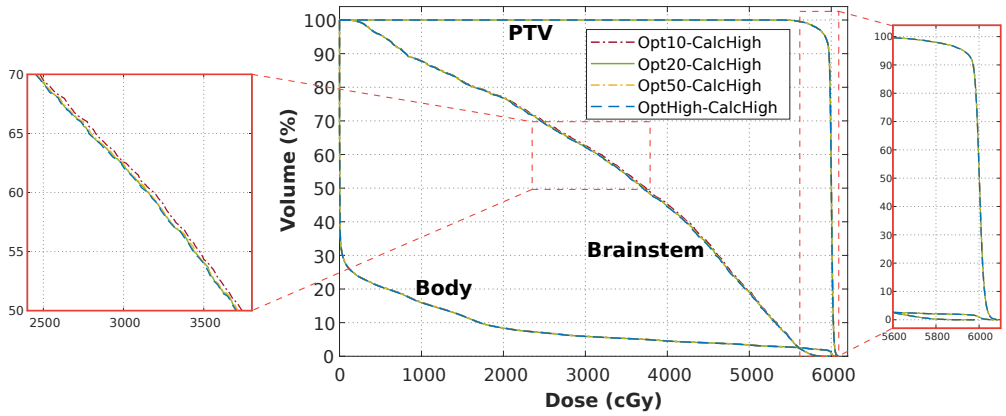

Case 1: Head Phantom

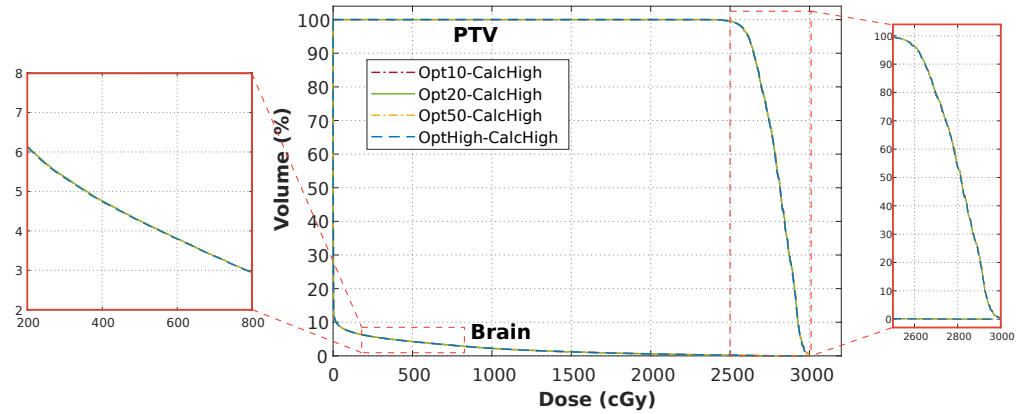

Case 2: Brain Metastasis

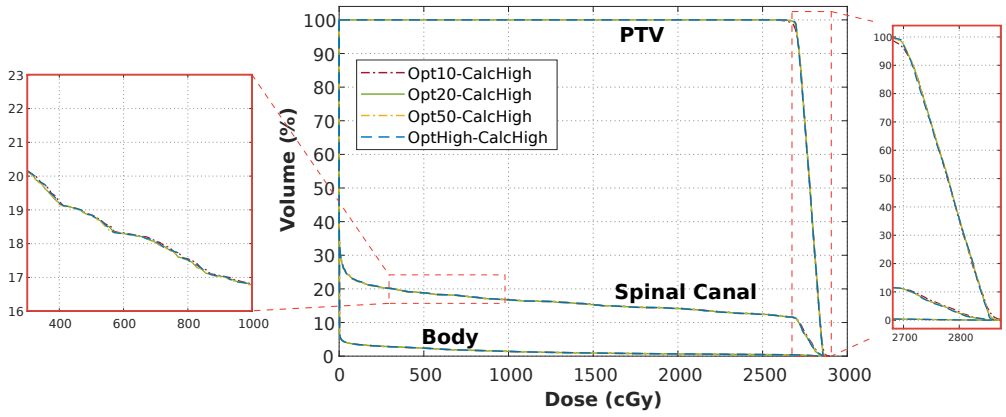

Case 4: Vertebral Metastases

Figure S2: Comparison of the DVHs for OARs and the target volume acquired from the standard and LDCTs showing the effect of CT dose reduction on plan optimization (OptLow-CalcHigh VS OptHigh-CalcHigh). Using LDCTs for plan optimization resulted in DVHs similar to the ground truth.

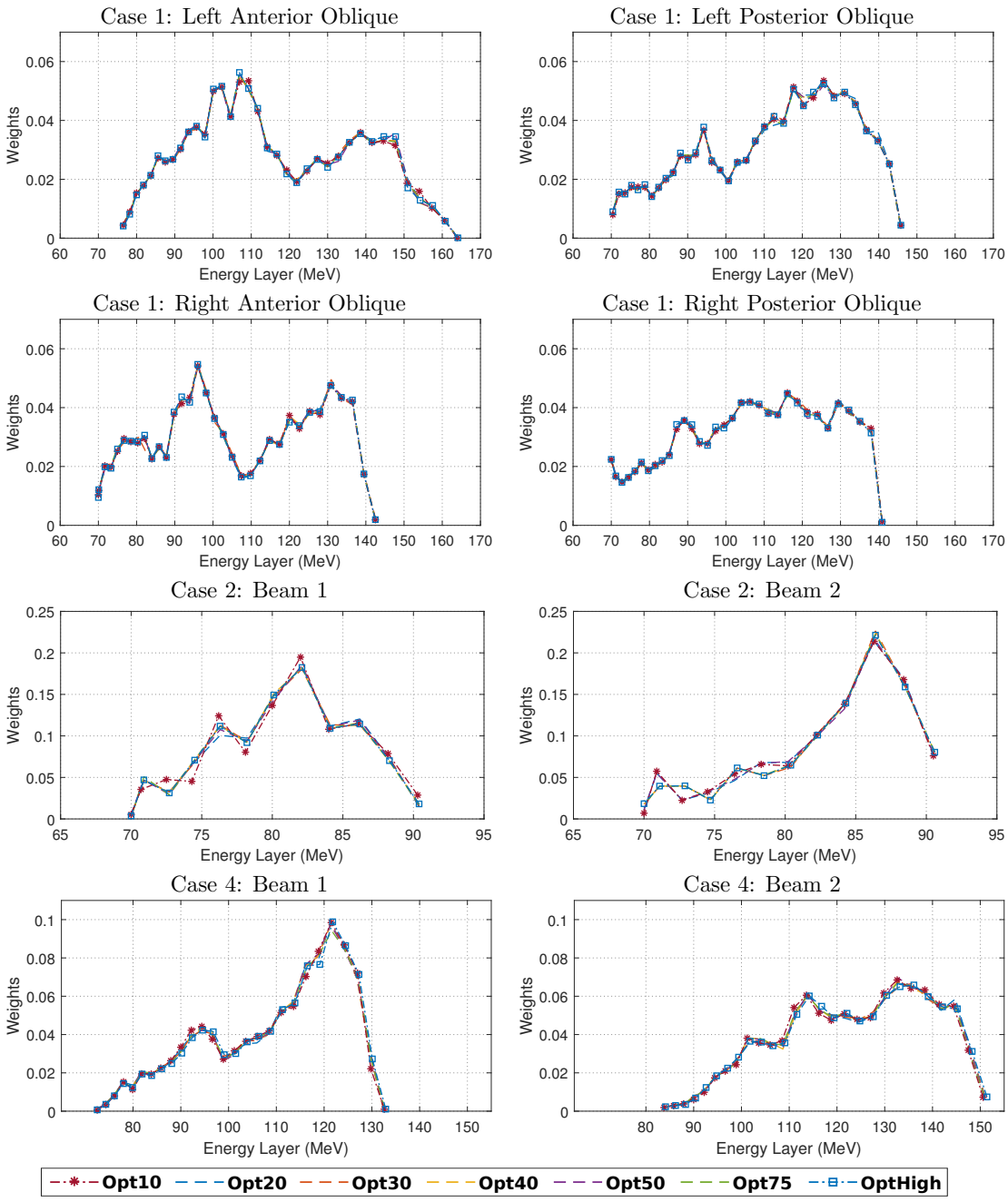

Figure S3: Representation of the energy layers and the corresponding relative weights. The plans are reoptimized on the standard-dose and LDCTs separately.

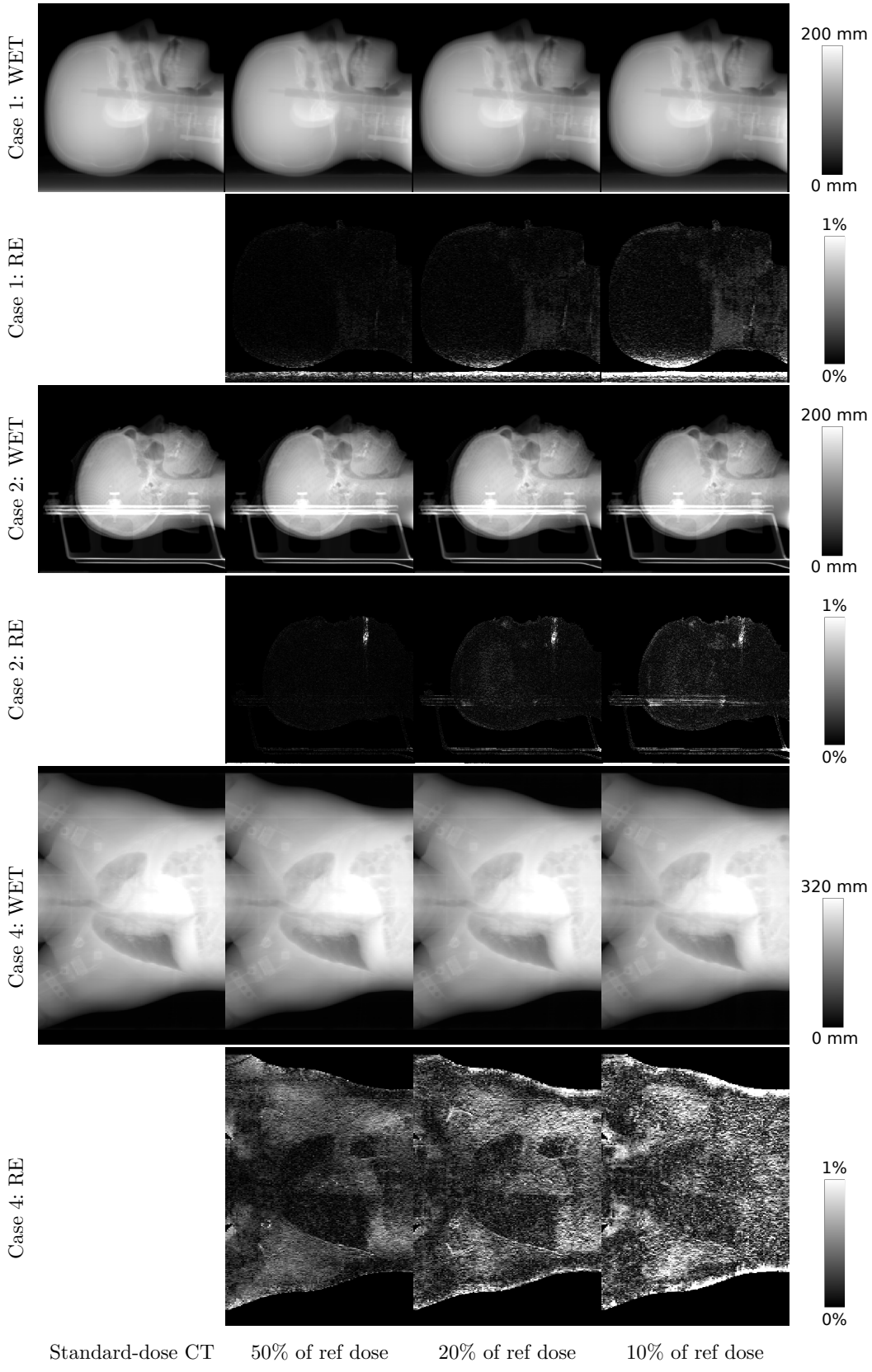

Figure S4: Representation of (first, third, and fifth rows) the WET maps calculated from the standard-dose and LDCTs and (second, forth, and sixth rows) the corresponding relative error (RE).